Article

How the Big Bang end up inside a Black Hole

Enrique Gaztanaga [1,2]

[1] Institute of Space Sciences (ICE, CSIC), 08193 Barcelona, Spain; gaztanaga@darkcosmos.com
[2] Institut d Estudis Espacials de Catalunya (IEEC), 08034 Barcelona, Spain

Abstract: The standard model of cosmology assumes that our Universe began 14 Gyrs (billion years) ago with a hot Big Bang expansion out of nothing. It can explain a vast range of different astrophysical data from a handful of free cosmological parameters. However successful this model is, we have no direct evidence or fundamental understanding of some key assumptions: low entropy start, Inflation, Dark Matter and Dark Energy. Here we present a simpler and more physical explanation for the same observations that do not require such assumptions or new laws of Physics. It is based on the evidence that we live inside a Black Hole (BH) of mass $M \simeq 5 \times 10^{22} M_\odot$, which we observed as cosmic acceleration. How did the Big Bang end up inside such a BH? We propose that 25 Gyrs ago, a very low density cloud with this mass collapsed and form a BH. The collapse continued inside until it reached neutron energy densities (GeV) over solar mass ($M_\odot$) causal regions that exploded, like supernovae, producing a bounce and the Big Bang expansion. During collapse, perturbations exit the horizon to re-enter during expansion, given rise to the observed universe. We review the theoretical and observational evidence for such BH Universe.

Keywords: Cosmology; Dark Energy; General Relativity; Black Holes

1. Introduction

A cosmological model predicts the evolution of the observed Universe given some initial conditions. The standard cosmological model [1,2], called Λ Cold Dark Matter (ΛCDM), assumes that our Universe began in a hot Big Bang expansion from almost nothing at the very beginning of space-time. The ΛCDM model explains the formation, composition and evolution of our Universe starting from a quantum fluctuation close to Planck scale. Planck scales are so small that space-time itself has to be treated as a quantum object. To address such initial conditions properly we need a new quantum theory of space-time (Quantum Gravity), which we don't yet have. Such initial conditions violate energy conservation and are very unlikely as they have a low entropy ([3,4]).

Despite these shortfalls, the ΛCDM model seems very successful. But at the cost of introducing three more exotic ingredients or mathematical tricks: Inflation, Dark Matter and Dark Energy, for which we have no direct evidence or understanding at any fundamental level. Are they windows for new discoveries, like String Theory or new forms of matter/energy, or a signal that the paradigm needs to be replaced? Can we choose some different initial conditions and reproduce the success of ΛCDM model without those exotic fixes and within the known laws of Physics?

Here we present a brief review that summarizes several recent papers[5–11] that suggest a simpler explanation: the Black Hole Universe (BHU). This review also includes some new results and ideas. Previous studies miss interpreted super horizon scales as scales that were outside the BHU. This is clarified here together with some new details regarding the Big Bounce and the observational interpretation of super horizon perturbations. In §2 we give a brief presentation of the ΛCDM model and its observational support. In §3 we present the BHU model using a Newtonian approach. This provides a non technical but accurate physical interpretation of the model and all its equations without any mathematical jargon. Appendix A-B presents a summary of the same BHU solution in the more rigorous GR approach. Appendix C present, for the first time, some simple considerations of the possible effect of rotation in the BHU solution. We end with a Summary and Discussion that includes a review of related literature and previous results and a comparison between models.

Preprints (www.preprints.org) | NOT PEER-REVIEWED | Posted: 31 January 2022 doi:10.20944/preprints202201.0459.v1

2. Observational evidence for ΛCDM

We briefly discuss here the main observational evidence of the ΛCDM focusing on why exactly it needs those fixes. This review is not exhaustive or include all the relevant references. It is just a brief introduction and further work can be found in the references within. We assume flat topology.

2.1. The expansion of the Universe and the FLRW metric.

In 1929 Edwin Hubble published [12] his famous diagram or linear relation (the Hublle law): $\dot{r} = Hr$ relating the radial distance r of 46 galaxies to their radial recession velocity $\dot{r} \simeq zc$, given by the redshift z and the speed of light c ($\dot{r}$ is the time τ derivative: $\dot{r} \equiv \frac{dr}{d\tau}$). Hubble used redshift z from galaxy spectra estimated and published by Vesto Slipher (1917) [13] and Cephid distances r developed by Henrietta Leavitt [14] and calibrated by E. Opik[15]. But it was George Lemaitre who first understood, in 1927 [16], the meaning of such discovery [17]: spacetime is expanding following the new theory of General Relativity (GR) by Albert Einstein [18].

But you do not actually need GR to figure out the expansion equations. On large scales, the observable Universe looks homogeneous and isotropic. This alone, tell us that a physical radial distance r has to scale as $r = a(\tau)\chi$, where $a(\tau)$ is a dimensionless scale factor and χ is a comoving coordinate, which is fixed ($\dot{\chi} = 0$) for any comoving observer like us, moving with the Universe. This is the Friedmann–Lemaitre–Robertson–Walker (FLRW) metric (i.e. Eq.A10). The observed expansion law follows from derivation: $\dot{r} = \dot{a}\chi = Hr$ where $H \equiv \dot{a}/a$ is the Hubble expansion rate. Nowadays H is measured to be $H_0 \simeq 70$ Km/s/Mpc, so a galaxy at $r \simeq 300$Mpc has a recession velocity of $\dot{r} \simeq 21,000$Km/s and a redshift $z \simeq 0.07$. The Universe was 7% smaller at the time the light from that galaxy was emitted, $\tau \simeq \frac{r}{c} = 92$Myr ago. The expansion time is $H_0^{-1} \simeq 14$Gyr.

Consider a spherically symmetric region of space $r < R$ with a fix mass M (like Lemaitre model [16]). We can use Gauss law (or Birkhoff theorem in GR [19]) to ignore what is outside R so the dynamics of R will be given by the free-fall equation:

$$E = \Phi + K = 0 \;\Rightarrow\; K = \frac{1}{2}\dot{R}^2 = \frac{1}{2}H^2R^2 = -\Phi = \frac{GM}{R} = \frac{4\pi G}{3}\rho R^2 \tag{1}$$

The above equation leads to Friedmann equation (i.e. Eq.A11), which is independent of R:

$$r_H^{-2} \equiv H^2(\tau) = \frac{8\pi G}{3}\rho(\tau) \tag{2}$$

At any time, the expansion rate H^2 is given by ρ. In our Universe we have measured their values today (ρ_0 and H_0) to find that they do follow: $H_0^2 = 8\pi G\rho_0/3$. We use units where the speed of light is $c = 1$, and $r_H \equiv H^{-1}$ is called the Hubble Horizon. Energy-Mass conservation requires $\rho \propto a^{-3(1+\omega)}$ where $\omega = p/\rho$ is the equation of state of the fluid: $\omega = 0$ for matter, $\omega = 1/3$ for radiation and $\omega = -1$ for vacuum. Given $a_* = a(\tau_*)$ at some reference time τ_* and $\tau = 0$ at $a = 0$, the solution to Eq.2 is:

$$H^2 = \left(\frac{\dot{a}}{a}\right)^2 = H_*^2\left(\frac{a}{a_*}\right)^{-3(1+\omega)} \Rightarrow a(\tau) = a_*\left[\frac{3(1+\omega)}{2}\tau H_*\right]^{\frac{2}{3(1+\omega)}} \Rightarrow r_H = \frac{3(1+\omega)}{2}\tau \tag{3}$$

During collapse H and τ are negative. Note that $r_H \propto a^{3(1+\omega)/2}$, so for regular matter ($\omega > 0$), it grows faster than comoving scales: $r = a\chi$ (the opposite is true for $\omega = -1$). Thus, for $\omega > 0$ all scales become super horizon ($r > r_H$) during collapse ($H < 0$) and re-enter the Hubble horizon during expansion. Also note that r_H increases with time τ (like the particle horizon). These equations are the exact solutions to GR for a FLRW metric, where τ is proper time for a comoving observer. Using Eq.2-3 we find:

$$\rho = \rho_0\left[\frac{3}{2}(1+\omega)\,H_0\tau\right]^{-2}. \tag{4}$$

which tell us what is the density at any time τ. In general ρ could be made of several components ρ_i: $\rho = \sum_i \rho_i$ each with different ω_i. The relative contributions are called cosmological parameters:

Preprints (www.preprints.org) | NOT PEER-REVIEWED | Posted: 31 January 2022 doi:10.20944/preprints202201.0459.v1

$\Omega_i \equiv \rho_i/\rho$, so that $\sum_i \Omega_i = 1$. As $\tau \Rightarrow 0$ the matter density becomes very high and the radiation density dominates and gets hot: $T = T_0/a$.

2.2. Nucleosynthesis and CMB.

In 1964, Penzias and Wilson [20] accidentally found a uniform Cosmic Microwave Background (CMB) radiation of temperature $T_0 \simeq 3K$. Robert Dicke, James Peebles, P. G. Roll, and D. T. Wilkinson in the companion publication [21] interpret this radiation as a signature from the Big Bang: the oldest light in the Universe. This was first noticed in 1948 by R.Alpher and R.Herman [22,23] who developed the theory of the primordial Nucleosynthesis and predicted a leftover CMB radiation of $T_0 \simeq 5K$, closed to the observed value. The idea behind is simple. Because the universe is expanding, when you imagine going back in time the density must get higher and higher, atoms will break and the resulting plasma will be dominated by radiation, like the interior of a star. If you simulate an expansion from such initial conditions you can build a prediction for the primordial abundance of elements and radiation that we observed today. This is called primordial Nucleosynthesis.

Hydrogen is the most abundant element measured in our Universe. Around $\sim 75\%$ of the total mass of the atoms (nucleons) in the Universe is in form of hydrogen, the remaining 25% is mostly Helium. The abundance predicted by Nucleosynthesis depends on the cross section of several Nuclear Physics reactions, like the neutron capture or decay. These are proportional to the ratio $\eta = \rho_B/\rho_R$ of the number density of baryons ρ_B (protons and neutrons) to that of photons, ρ_R, given by the CMB background temperature $T = T_0/a$. So a measurement of the primordial element abundance and ρ_B can be used to predict T_0. Nowadays we use the more precise measured value $T_0 = 2.726K$ and the observed abundance to predict ρ_B. In relative units: $\Omega_B = \rho_B/\rho \simeq 0.05$ [24]. So that only $\simeq 5\%$ of the total energy-density in our Universe is made or regular matter (i.e. made of known baryons and leptons). The rest, according to ΛCDM , is made of Dark Matter and Dark Energy.

2.3. Cosmic Inflation and the horizon problem.

Cosmic Inflation[25–28] consists of a period of exponential expansion that must happened right after the beginning of time ($\tau = 0$). There are over a hundred versions and variations [2,29], but generically the model requires some hypothetical new scalar field (the inflaton) with negligible kinetic energy ($\omega = -1$) to dominate the very early universe. After expanding by a factor e^{60}, inflation leaves the universe empty and we need a mechanism to stop inflation and create the matter and radiation that we observe today. This is called re-heating. All these components require some fine tuning and free parameters. But Inflation solves some important mysteries that we don't know how to fix otherwise within ΛCDM .

As mentioned below Eq.3, the structures that we observed today were not in causal contact in the past. We say that they were super horizon. Structures that are larger than r_H can not evolve because the time a perturbation takes to travel that distance is larger than the expansion time. How can these structures form if they were not in causal contact? This is the horizon problem. A clear evidence of this problem is the uniform CMB temperature across the full sky. The Hubble horizon r_H at CMB times only subtends about one degree in our sky. So causality can not explain the observed all sky CMB uniformity. The horizon problem is solved by inflation because during inflation structures of all scales become super horizon. After inflation ends, they re-enter the horizon ($\omega = -1$). Moreover reheating provides a very uniform temperature background at the end of inflation.

2.4. Structure formation and Dark Matter.

In 1992, NASA's Cosmic Background Explorer (COBE) satellite detected temperature variations of very small relative amplitude $\delta_T \simeq 10^{-5}$ in the CMB [30]. We believe those were the seeds that grew under gravitational collapse to form star, galaxies and the cosmic web that we observe today. But where do the seeds come from? Models of Inflation propose that these seeds come from super horizon quantum fluctuations that were exponentially inflated during inflation. Inflation predicts a power law (almost scale invariant) spectrum of fluctuations which agrees with the shape measured

Preprints (www.preprints.org) | NOT PEER-REVIEWED | Posted: 31 January 2022 doi:10.20944/preprints202201.0459.v1

by later CMB missions [31–34] and clustering in Galaxy Surveys [35–38]. But Inflation does not provide a specific prediction for $\delta_T \simeq 10^{-5}$: it is just a free parameter of the model.

The measured $\delta_T \simeq 10^{-5}$ is too small to explain the observed structure in galaxy surveys today [39]. Some fix is needed: galaxy bias [40,41] or a Λ term [35]. The shape of the spectrum of fluctuations (including the Baryon Acoustic Oscillations, BAO [42–45]) in the CMB and Galaxy Surveys, also required another free component to agree with the ΛCDM model. They require a new type of matter, that we called Cold Dark Matter (CDM[46]) which is not made of regular matter (baryons) and interacts very weakly with matter or radiation (thus the name). CDM needs to be about 4 times more abundant than regular matter: $\Omega_{CDM} \simeq 4\Omega_B$. Such CDM is also needed to understand the motion of galaxies in clusters [47], the galaxy rotational curves [48], gravitational lensing[49], galaxy evolution[46], cosmic flows[50] and structure in galaxy maps[35–38]. Despite enormous observational efforts in the last 30yrs, such Dark Matter component has never been directly detected as a real particle or object.[51,52]

2.5. Cosmic acceleration,Dark Energy and the static universe

Usually cosmic acceleration is defined by the adimensional coefficient $q \equiv (\ddot{a}/a)H^{-2}$. Taking a derivative to Eq.3 we find $q = -\frac{1}{2}(1+3\omega)$. For regular matter we have $\omega > 0$ so we expect the expansion to decelerate ($q < 0$) because of gravity. But the latest concordant measurements from Type Ia supernova (SN)[53,54], galaxy clustering and CMB all agree with an expansion that tends to $\omega = -1.03 \pm 0.03$ [38] or $q \simeq 1$ in our future.

Dark Energy (DE) was introduced [55] to account for $\omega < 0$. But there is no fundamental understanding of what DE is or why $\omega \simeq -1$. A natural candidate for DE is the cosmological constant Λ [56–59] which has $\omega = -1$ and can also be thought as the ground state of a scalar field (the DE), similar to the Inflaton. Λ can also be a fundamental constant in GR, but this has some other complications [57–59]. Including DE in the ΛCDM model is also needed to complete the energy budget for our Universe: 5% baryons ($\Omega_B \simeq 0.05$), 25% Dark Matter ($\Omega_{DM} \simeq 0.25$) and 70% DE ($\Omega_\Lambda \simeq 0.7$), so that $\Omega_B + \Omega_{DM} + \Omega_\Lambda = 1$, as needed. DE is also important to understand the Integrated Sachs-Wolfe (ISW) effect[60,61], and to have a longer age estimate of 14 Gyr, which is needed both to account for the oldest stars and to have more time for structures to grow from the small CMB seeds $\delta_T \simeq 10^{-5}$ to the amplitude (and shape) we observe today in Galaxy Maps [35,39].

Note how $q = 1$ means $\dot{H} = 0$, so that H becomes constant and all structures becomes super horizon and freeze, like in Inflation. In the physical frame (see §A.1) this corresponds to a static (deSitter) metric. We are used to repeat that the universe accelerates, but in the limit $q \Rightarrow 1$ it is more physical to say that the universe becomes static, as proposed by Einstein [56] when he introduced Λ.

3. Inside a Black Hole (BH)

A BH is defined as an object with a radial escape velocity $\dot{r} = c \equiv 1$. The escape velocity $\dot{r}$ is the minimum one needed to just escape the gravitational pull of a mass M. This requires: $\frac{1}{2}\dot{r}^2 = \frac{GM}{r}$. Thus, for a BH we have that $r \equiv r_S = 2GM$, which is called the Event Horizon. According to relativity, events can not travel faster than c, which means that nothing can escape from inside r_S. The density and mass of a BH just depends on r_S, and its radius and mass only depends on its density:

$$\rho_{BH} = \frac{M}{V} = \frac{3M}{4\pi r_S^3} = \frac{3r_S^{-2}}{8\pi G} \tag{5}$$

This is the exact density of our Universe in Eq.2 inside its Hubble Horizon $r_H = 1/H$, as for $r = r_H$ the expansion law gives: $\dot{r} = Hr = 1$. Perturbations larger than r_H (called super horizon) cannot evolve because the time a perturbation takes to travel that distance is larger than the expansion time. So the Hubble volume around us ($r < r_H$) is causally disconnected from the rest ($r > r_H$) and has the density of a BH. Another way to define the Event Horizon at time τ is by the maximum distance r_* that light can travel given infinite time[62]. The FLRW event Horizon is then:

$$r_* = a\int_\tau^\infty \frac{d\tau}{a(\tau)} = a\int_a^\infty \frac{d\ln a}{aH(a)} < \frac{1}{H_\Lambda} \equiv r_\Lambda \tag{6}$$

Preprints (www.preprints.org) | NOT PEER-REVIEWED | Posted: 31 January 2022 doi:10.20944/preprints202201.0459.v1

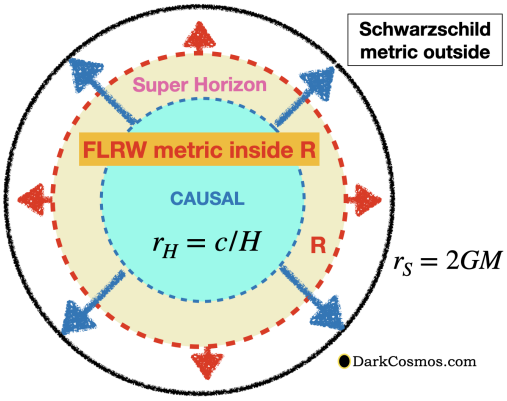

Figure 1. Illustration of our Universe inside the event horizon $r_S = 2GM$. This is a Schwarzschild (empty) metric outside ($r > R$) and a FLRW metric inside R (red dashed line) with mass M. The Hubble radius $r_H = c/H$ (dashed line) defines the volume inside causal contact (blue shading). The BHU solution in Eq.8 requires $R = [r_H^2 r_S]^{1/3}$, so that R grows slower than r_H. There is a region with matter outside the Hubble radius $R > r > r_H$ (yellow shading) with super horizon (or frozen) perturbations. This solves the horizon problem in Cosmology and is a source for perturbations that enter the horizon as the metric expands, creating LSS and BAO in Cosmic Maps, pretty much like what is usually assumed for Cosmic Inflation.

where we have used the observational fact [38] that H tends to a constant $H_\Lambda = H_0\Omega_\Lambda^{1/2}$ in our future. This means that $r_S = r_\Lambda = 2GM$. No signal from inside r_* can escape outside. So we do live inside a BH of size:

$$r_S = 2GM = r_\Lambda \equiv H_\Lambda^{-1} = H_0^{-1}\Omega_\Lambda^{-1/2} \quad \Rightarrow \quad M \simeq 5\times 10^{22} M_\odot \tag{7}$$

where $\Omega_\Lambda \simeq 0.7$ and $H_0 \simeq 70$ Km/s/Mpc. If we use $r_S = 2GM$ in Eq.1 we find:

$$R = [r_H^2 r_S]^{1/3} \Rightarrow R(\tau) = \frac{3(1+\omega)}{2}\tau_*^{1/3}\tau^{2/3} = r_S\left(\frac{a}{a_{BH}}\right)^{1+\omega} \tag{8}$$

where a_{BH} is the scale factor when the BH event horizon is reached. This equation give us the evolution of a finite FLRW cloud radius $R(\tau)$. Compared to Eq.3 we can see that R grows slower than r_H so perturbations become superhorizon during collapse and re-enter during expansion. So the collapsing phase acts like Inflation. In units of r_H today $c/H_0 \equiv 1$, at CMB times ($a \simeq 10^{-3}$): $r_H \simeq 5\times 10^{-5}$, while R is about 30 times larger. For constant $H = H_\Lambda$ we have $R = r_S$, which is larger than R_0 today. Thus we are inside a BH. Note how for $R < r_S$ (i.e. inside the BH) Eq.8 indicates that there is a region with no matter: $r_S > r > R$ and a region with matter outside the Hubble horizon $R > r > r_H$. This is illustrated in Fig.1.

Here we have obtained Eq.2 and Eq.8 just using Newtonian Mechanics with the definition of a BH. This is the same solution as the BH Universe (BHU)[8], which is an exact solution to GR and corresponds to a FLRW cloud as in Eq.1. Appendix A presents this exact BHU solution within GR.

3.1. How did we end up inside a BH?

Our Universe must have collapsed from to form one! Before it collapsed, the density of such a large BH in Eq.7 is so small that there are no interactions other than gravity. Any radiation will escape the cloud, but the collapse of its matter is unavoidable. This also happens with regular stars. We take τ_* in Eq.3 to correspond to the time τ_{BH} when $r_H = -r_S$, i.e. FLRW cloud formed a BH:

$$\tau_{BH} = \tau_* = -\frac{2}{3(1+\omega)}r_S \simeq -11 Gyrs \tag{9}$$

where we have used Eq.7 and $\omega \simeq 0$ during the most part of the collapse (the latest stages of the collapse have $\omega \simeq 1/3$, but they last a negligible time compare to matter domination). Thus the BH forms 11 Gyr before $\tau = 0$ (the Big Bang) or 25Gyr ago. The collapse continued after the BH formation. In the last stages of the collapse atoms ionized and part of the energy transforms into

Preprints (www.preprints.org) | NOT PEER-REVIEWED | Posted: 31 January 2022 doi:10.20944/preprints202201.0459.v1

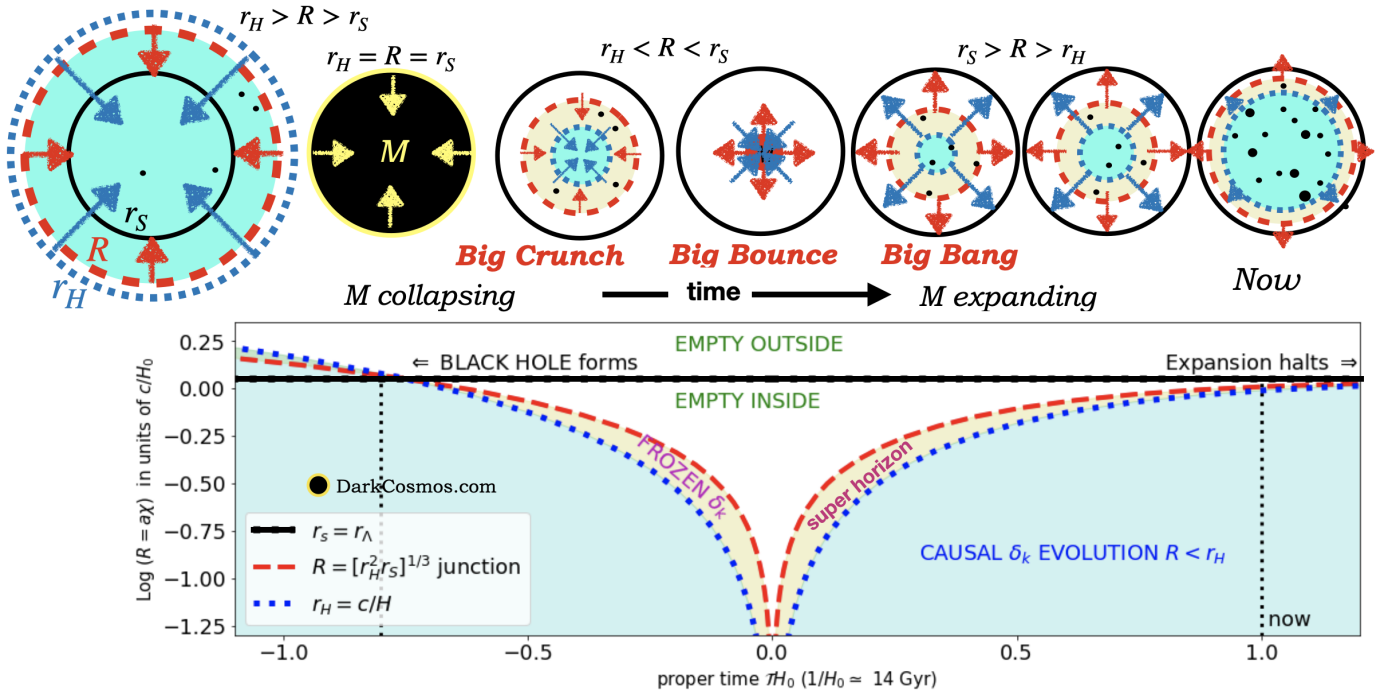

Figure 2. Physical coordinate radius R collapsing and expanding as a function of comoving time τ. A spherical cloud of radius R and mass M starts collapsing free-fall under its own gravity. When it reaches $R = r_S = 2GM$ it becomes a BH (black sphere). The collapse proceeds inside the BH until it bounces into an expansion (the hot Big Bang). The BH Event Horizon r_S behaves like a cosmological constant with $\Lambda = 3/r_S^2$ so that the expansion freezes before it reaches back to r_S. Blue shading ($R < r_H$) indicates causal evolution of perturbations. White is approximated as empty space. Super horizon structures in-between R and r_H (yellow shading) are "frozen" and they seed structure formation as they re-enter r_H. Contrary to Inflation, the super horizon spectrum of perturbations in the BHU has a cut-off at scales at R.

heat. Radiation pressure will soon dominate the resulting plasma like in the interior of a star. This slows down the collapse. Fig.2 shows the numerical BHU solution using Eq.3 and Eq.8.

3.2. The Big Crunch

As mentioned before, there is a region outside the Hubble Horizon $R > r > r_H$ which is dynamically frozen (yellow shading in Fig.1-2). This is the source for super horizon perturbations, which can be observed today in the CMB temperature maps. Any small irregularities $\delta \equiv \Delta\rho/\rho$ (like the particle composition of the fluid) will grow under gravity. This is the so call gravitational instability. The growth of δ can start early on within the FLRW cloud, well before τ_{BH}. The amplitude of δ from gravitational instability is scale invariant [63–65]. In the linear regime, δ follows a damped harmonic oscillator equation whose solutions [66] are $D_+ \propto a$ and $D_- \propto a^{-3/2}$, which correspond to the growing and decaying mode during expansion. In the collapsing phase the damping term has a negative sign and fluctuations grow faster with time because D_- is the growing mode when a goes to zero. It is therefore likely that galaxy, stars, planets or life could also form during the collapsing phase. The details might depend on the original FLRW cloud composition. As the cloud collapses and the background density increases the structures will disappear inside a hot Big Crunch, but the largest scale density perturbations will become super horizon (freeze out) and survive the Big Bounce, as they correspond to small variations of the background over large scales.

3.3. The Big Bounce

The energy density is given by Eq.4 which is homogeneous everywhere. By $a \simeq 10^{-12} a_{BH}$ or $\tau \simeq -10^{-4}$ seconds, the energy density becomes that of a neutron star $\rho(n^o)$ (GeV). The Hubble radius at that time $r_H \simeq 30$Km corresponds to a solar mass, so the situation is similar to the interior of a collapsing star. We conjecture that this leads to Big Bounce, either because of supernova

Preprints (www.preprints.org) | NOT PEER-REVIEWED | Posted: 31 January 2022 doi:10.20944/preprints202201.0459.v1

explosion or because of the elasticity of the neutron density [67]. This generates a hot Big Bang from the Big Crunch, similar to the bouncing of a ball.

Neutron density corresponds to the highest stable density observed in nature for a star. This indicates that something prevents higher densities. Each r_H region is causally disconnected and evolves independently of the rest. If the neutron material is elastic enough the collapse could just bounce into an expansion. This works pretty much like a bouncing of a ball. But if the expansion rate is too high, the collapse could led to a supernova (SN) explosion. Global rotation of the FLRW cloud could slow down the expansion rate (see Appendix C) and play some role in the impact of elasticity.

Stars explode as supernovas (SN) either because of runaway nuclear reactions or because of gravitational core-collapse. Protons and neutrons combine to form neutrons and neutrinos by electron capture. The gravitational potential energy Φ of the collapse is converted into a neutrino burst. Neutrinos are reabsorbed by the infalling layers producing an SN explosion. For example, the Crab Nebula pulsar in Fig.3 is thought to be a core collapse supernova that exploded releasing a total energy of $10^{51} - 10^{52}$ ergs in the explosion. This energy is very similar to the FLRW collapsed energy of a $M_\odot$ star within $r_H \simeq 30$Km. Recall that the collapse speed is c for r_H, so this is also closed to the internal (or rest) energy in Einstein's most famous equation: $E = M_\odot c^2$.

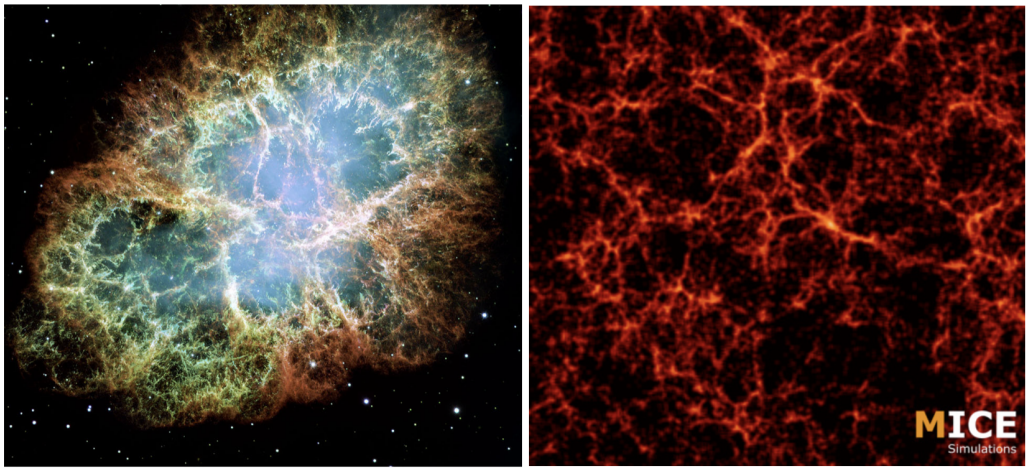

Figure 3. LEFT: The Crab Nebula explosion as observed in 1999 from the Hubble Space Telescope, 945yrs after it exploded. A pulsar remnant could be part of the Dark Matter. RIGHT: the MICE simulation[68] of our expanding Universe. The resulting structures look similar. Both are related in the Big Bounce model.

Both SN or elastic reactions are synchronized at different locations because the background density is the same (at any given proper time τ) everywhere in the FLRW cloud. The collapse energy is converted into expansion energy. This is the same FLRW metric we had in the collapse but with $H > 0$. Neutron stars, pulsars and small primordial BHs (PBHs[69]) could result as remnants of the SN explosions and they could contribute to the Dark Matter that we see today. The bounce happens at times and energy densities which are many orders of magnitudes away from Inflation or Planck times ($\tau \simeq 10^{-35}$). So Quantum Gravity is not needed to understand the Big Bounce and there is no monopole problem[26]. The idea needs to be worked out and simulated, but a Big Bang from a Big Bounce seems more plausible that one that comes out of nothing.

3.4. The horizon problem

The farther back we observe an image in the sky, the older it is. The Big Bang, if we could see it, corresponds to a very distant spherical shell in the sky, represented by large red circles in Fig.4. The furthest we can actually see is the CMB shell (dashed circle), which is quite close to $\tau = 0$. This means that r_H (or corresponding comoving particle horizon χ) subtends a very small angle in the sky. So no physical mechanism can create the uniform CMB temperature that we see across the full sky. The initial conditions in the Big Bang have to be uniform to start with. This is very unlikely if the Big Bang came out of nothing[3,26]. But is exactly what we expect if the Big Bang originates from a uniform Big Bounce. This provides a solution to the Horizon problem without Inflation.

Preprints (www.preprints.org) | NOT PEER-REVIEWED | Posted: 31 January 2022 doi:10.20944/preprints202201.0459.v1

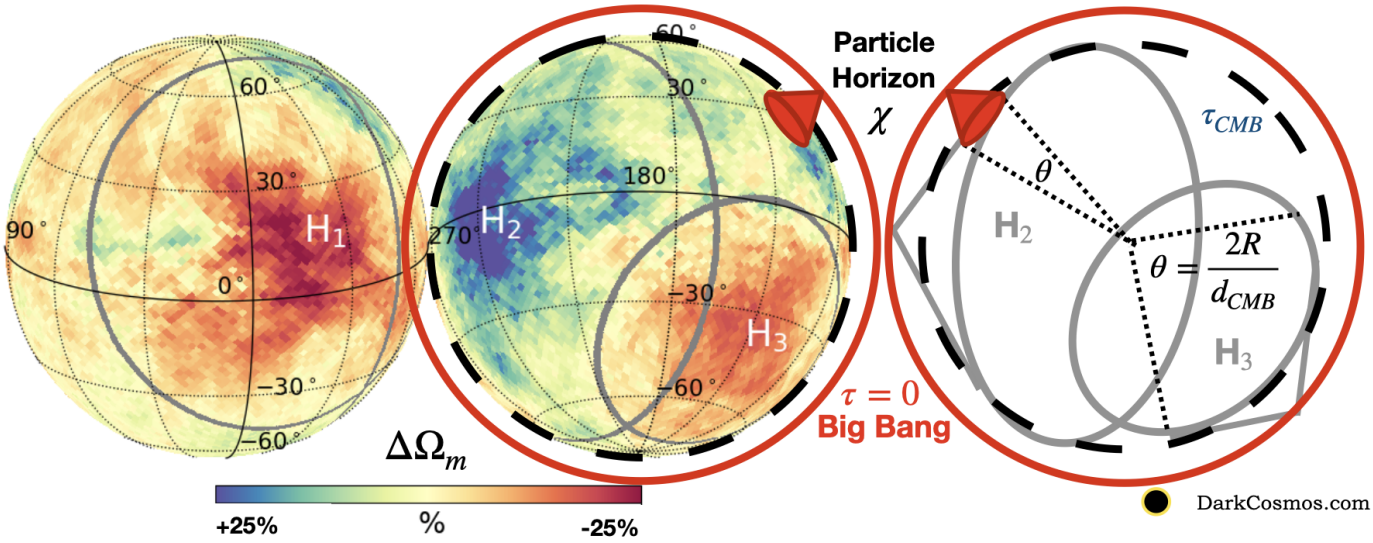

Figure 4. The CMB sky represented as the surface of a sphere (two view angles) whose radius is the distance traveled by the CMB light to reach us (at the center of the sphere). The red circle represents the corresponding spherical surface from the Big Bang light ($\tau = 0$), if we could see it. The CMB particle horizon $\chi \sim r_H$ (small red cones) is the distance travel by light between $\tau = 0$ and τ_{CMB} and subtends a very small angle in the observed CMB sky. Large grey circles on the CMB surface are therefore super-horizon boundaries (labeled H_1, H_2 and H_3) in the relative variations of cosmological parameters (color scale) at different locations of the CMB sky [7]. Regions H_i correspond to a cutoff in super horizon perturbations (of size $\theta \simeq 2R/d_{CMB} \simeq 60$deg.) out of the $\tau = 0$ surface. They are inside our BHU, but not causally connected (yellow region in Fig.2).

After the Big Bang, the resulting radiation and plasma fluids cool down following the standard FLRW evolution (Nucleosynthesis and CMB recombination). The Big Bounce has super horizon irregularities from the collapsing phase which re-enter the horizon r_H as the expansion proceeds. These are the seeds for new structure (BAO and galaxies) that grow under gravitational instability, as illustrated in Fig.3. The key difference with Inflation is that in the BHU the spectrum of incoming fluctuations have a cutoff for scales larger than $\lambda > 2R$ ($k < \pi/R$), while Inflation is scale invariant in all scales. This results in anomalous lack of the largest structures in the CMB sky temperature T with respect to the predictions of Inflation. This particular CMB anomaly is well known but often interpreted in different ways [31,70–73].

A related anomaly is shown in Fig.4. It displays a sky map of relative variations in the fitted values of ρ_m (or cosmological parameter $\Omega_m = \Omega_B + \Omega_{DM} = 1 - \Omega_\Lambda$) over large regions around each position in the sky. There is a characteristic cutoff scale (or causal horizon) shown by grey circles labeled H_i. Same horizons are found for different cosmological parameters. This can be interpreted as a detection of super horizon fluctuations from the Big Bounce, with a cutoff given by the size of H_i. In Fig.5 we compare the different cutoff scales with the predictions of the BHU. There is a good agreement for both comoving scales χH_0 (left panel) and angular scales. These are independent because only the former depends on the measured values of H_0 in each horizon. A recent study of the homogeneity index in the CMB [10], finds a cutoff scale $\Theta_H = 66 \pm 9$ degrees. This is shown as the black symbol in Fig.5 for the mean values of $\Omega_m = 0.3$ and $H_0 = 67$ Km/s/Mpc in the full CMB sky.

3.5. Dark Energy

During the expanding phase we need to include Ω_Λ in the dynamics because the BH Event Horizon r_S forbids anything to escape. This appears in the action of GR as a Gibbons-Hawking-York (GHY) boundary term [74–76], which is equivalent to a Λ term when the evolution happens inside an expanding BH (see Appendix B). The measured Λ term is the Event Horizon of our BHU in Eq.7. In the standard Big Bang model there is no reason for cosmic acceleration. A new exotic ingredient, Dark Energy (DE), has to be added to account for this new evidence. Moreover, there is no fundamental understanding as to why the DE equation of state $\omega \equiv \rho/p$ should be so close to $\omega = -1$ as found by the latest data compilations [38]. This is instead the natural outcome of the BHU

Preprints (www.preprints.org) | NOT PEER-REVIEWED | Posted: 31 January 2022 doi:10.20944/preprints202201.0459.v1

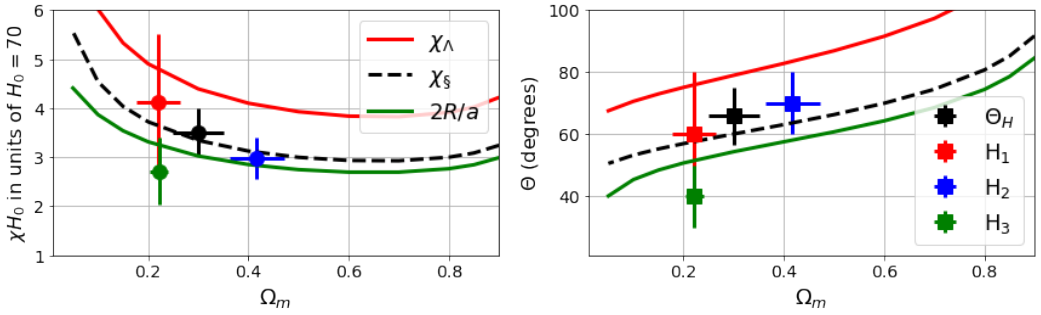

Figure 5. Comparison of the causal horizon H_i sizes shown in Fig.4 and θ_H from the homogeneity index [10] in comoving χH_0 and angular units, given the mean measured Ω_m and H_0 in each horizon. This is compared to the BHU predictions ($2R/a$, green), $\chi_\S$[6] (dashed) and $\chi_\Lambda = r_S/a$ (red) as a function of Ω_m.

because $\omega = -1$ corresponds to a constant BH Event Horizon $r_S = r_\Lambda$. The expansion freezes and becomes static in the physical frame. For a comoving observer this looks like exponential inflation, but both pictures are equivalent [8,77]. As in the standard cosmological model, it takes 14 Gyrs to reach now (or H_0) from the Big Bounce.

Discusion & Conclusion

Inflation is believed to solve the flatness problem: why our universe has a flat global topology (or geometry) $k = 0$? But given some matter content, GR can not give us its topology. This is a global property of spacetime that is either assumed or directly measured. The same applies to an intrinsic Λ term. Eq.2 and 8 in the BHU are also exact solutions in GR for $k \neq \Lambda \neq 0$ by just replacing $r_H^{-2} \equiv H^2 + k/a^2 + \Lambda/3$. But we use $k = \Lambda = 0$ here because these are the values in empty space (for Minkowski metric) and there is no reason, within GR, that they should be different in the presence of matter. So we believe there is no flatness or Λ problem that needs to be solved.

The ΛCDM model interprets cosmic acceleration as evidence for Dark Energy (or an intrinsic Λ term). We propose instead that this is an indication that we live inside a BH. This results in the BHU solution to GR (see Appendix A), which we have reproduced here in Eq.8 using simple Newtonian physics. The idea that the universe might be generated from the inside of a BH is not new and has extensive literature[78–82] which mostly focused in deSitter metric for the BH interior. The formation mechanisms involve some modifications or extensions of GR, often motivated by Quantum Gravity or String Theory. The BHU solution is also similar to the Bubble Universe and gravastar solutions [83–88]. But there are no surface terms (or Bubble) in the BHU and there is regular matter and radiation inside (see Appendix A). Several authors before have proposed that the FLRW metric could be the interior of a BH [89–93]. But these solutions were incompleted [94] or outside GR. Stuckey[95] showed that a dust filled FLRW metric can be formally joined or glued to an outside BH metric, which is an independent precursor to the BHU model.

The measured cosmic acceleration give us the exact value for the Event Horizon r_S in Eq.7. Such interpretation provides a fundamental explanation to the meaning of Λ (see also Appendix B). This leads to a Big Bounce in Fig.2, which provides a uniform start for the Big Bang, solving the horizon problem. The yellow shaded regions in Fig.12 indicate that a large fraction of the mass M that collapsed into our BHU moved outside the horizon r_H. Super horizon perturbations can then be the seeds to structure (BAO and galaxies) as they re-enter r_H, in a similar way as is proposed by models of Inflation. The main differences with Inflation is the origin of those perturbations and the existence of a cutoff in the spectrum of fluctuations given by $R(\tau)$. As illustrated in Fig.4-5, such cutoff has recently been measured in the CMB maps [7,10]. Current and future galaxy surveys are also able to measure this signal [36,37]. The existence of super horizon perturbations could also be related to the tension in measurements of cosmological parameters from different cosmic scaletimes [96–98] which have similar variations in cosmological parameters[7]. The Big Bounce could also help us understand two remaining mysteries in the ΛCDM paradigm: the origin for the amplitude $\delta_T \simeq 10^{-5}$ in the CMB and the nature of Dark Matter. Structure formation during the collapse could be key to understand them. Remnants from supernova explosions, such as BH, neutron stars or pulsars, during the Big Bounce could also be detected and account for Dark Matter. Is there any evidence for what is outside the BHU? In Appendix C we give some simple considerations on how BH rotation could play a role. All these ideas requires further work. Table 1 presents a comparison of ΛCDM and BHU solutions.

The BHU solution can also be used to understand the interior of a BH. This sounds similar to Smolin[99], who speculated that all final (e.g. BH) singularities 'bounce' or tunnel to initial singularities of new universes. But the bounce proposed here, avoids both the BH and the Big Bang mathematical singularity theorems[100,101]. That a non singular version of such solutions exist is clear from direct observations. As stated by Ellis[102], the concept of physical infinity is not a scientific one. The Big Bounce also avoids the entropy paradox[3] in the Big Bang model in a similar way as proposed by Penrose [4], but just using the known laws of physics

Preprints (www.preprints.org) | NOT PEER-REVIEWED | Posted: 31 January 2022 doi:10.20944/preprints202201.0459.v1

Table 1: Model comparison. Observations that require explanation.

Cosmic observation	ΛCDM explanation	BHU explanation
Expansion law	FLRW metric	FLRW metric
Element abundance	Nucleosynthesis	Nucleosynthesis
Cosmic Microwave Background (CMB)	recombination	recombination
All sky CMB uniformity	Inflation	Uniform Big Bounce
CMB fluctuations $\delta T = 10^{-5}$	Inflation	Big Crunch perturbations
Cosmic acceleration, BAO & ISW	Dark Energy ($\Lambda \neq 0$)	BH event horizon
14Gyr age to $\tau = 0$	Dark Energy ($\Lambda \neq 0$)	BH event horizon
Rotational curves & Cosmic flows	Dark Matter	BHs, pulsars remnants of Big Bounce
$\Omega_m \simeq 4\Omega_B$ & gravitational lensing	Dark Matter	BHs, pulsars remnants of Big Bounce
Large scales anomalies in CMB	Cosmic Variance (bad luck)	super-horizon cutoff $\lambda < 2R$
anomalies in cosmological parameters	Systematic effects	super-horizon perturbations
flat universe $k = 0$	Inflation	Minkowski metric
monopole problem	Inflation	low energy Big Bounce

and without cyclic repetition, as it takes infinite proper time to reach r_S. Our Universe will end up trapped, static and frozen, just as first modeled by Einstein in 1917[56] when he introduced Λ. But Λ is just the Event Horizon of our BHU and therefore of a larger and older universe.

Acknowledgments: I would like to thank Benjamin Camacho, Pablo Fosalba, Nanda Rea, Facundo Rodriguez and Santi Serrano for comments on the original manuscript. This work has been supported by spanish MINECO grants PGC2018-102021-B-100 and EU grants LACEGAL 734374 and EWC 776247 with ERDF funds. IEEC is funded by Generalitat de Catalunya.

Conflicts of Interest: The authors declare no conflict of interest.

References

1. Dodelson, S. *Modern cosmology, Academic Press, NY*; 2003.
2. Weinberg, S. *Cosmology, Oxford University Press*; 2008.
3. Dyson, L.; Kleban, M.; Susskind, L. Disturbing Implications of a Cosmological Constant. *J.of High Energy Phy* **2002**, *2002*, 011.
4. Penrose, R. Before the big bang: An outrageous new perspective and its implications for particle physics. *Conf. Proc. C* **2006**, *060626*, 2759–2767.
5. Gaztañaga, E. The size of our causal Universe. *MNRAS* **2020**, *494*, 2766–2772.
6. Gaztañaga, E. The cosmological constant as a zero action boundary. *MNRAS* **2021**, *502*, 436–444.
7. Fosalba, P.; Gaztañaga, E. Explaining cosmological anisotropy: evidence for causal horizons from CMB data. *MNRAS* **2021**, *504*, 5840–5862.
8. Gaztanaga, E. The Black Hole Universe (BHU) from a FLRW cloud. submitted to Physics of the Dark Universe, hal-03344159.
9. Gaztanaga, E. The Cosmological Constant as Event Horizon. *Universe* **2022**, *in press*.
10. Camacho, B.; Gaztañaga, E. A measurement of the scale of homogeneity in the Early Universe. *arXiv:2106.14303* **2021**.
11. Gaztañaga, E.; Fosalba, P. A peek outside our Universe. *Symmetry in Press* **2022**, p. arXiv:2104.00521.
12. Hubble, E. A Relation between Distance and Radial Velocity among Extra-Galactic Nebulae. *Proc. N.A. of Science* **1929**, *15*, 168–173.
13. Slipher, V.M. Radial velocity observations of spiral nebulae. *The Observatory* **1917**, *40*, 304–306.
14. Leavitt, H.S.; Pickering, E.C. Periods of 25 Variable Stars in the Small Magellanic Cloud. *Harvard College Obs.Circular* **1912**, *173*, 1–3.
15. Opik, E. An estimate of the distance of the Andromeda Nebula. *ApJ* **1922**, *55*, 406–410.
16. Lemaître, G. Un Univers homogène de masse constante et de rayon croissant rendant compte de la vitesse radiale des nébuleuses extra-galactiques. *Annales de la S.S. de Bruxelles* **1927**, *47*, 49–59.
17. Elizalde, E. *The True Story of Modern Cosmology: origins, main actors and breakthroughs*; Springer, 2021.
18. Einstein, A. Die Grundlage der allgemeinen Relativitätstheorie. *Annalen der Physik* **1916**, *354*, 769–822.
19. Deser, S.; Franklin, J. Schwarzschild and Birkhoff a la Weyl. *American Journal of Physics* **2005**, *73*, 261–264.
20. Penzias, A.A.; Wilson, R.W. A Measurement of Excess Antenna Temperature at 4080 Mc/s. *ApJ* **1965**, *142*, 419–421.
21. Dicke, R.H.; Peebles, P.J.E.; Roll, P.G.; Wilkinson, D.T. Cosmic Black-Body Radiation. *ApJ* **1965**, *142*, 414–419.
22. Alpher, R.A.; Herman, R.C. On the Relative Abundance of the Elements. *Physical Review* **1948**, *74*, 1737–1742.
23. Alpher, V.S. Predicting the CMB: The hazards of being first. *Physics Today* **2015**, *68*, 10–10.
24. Steigman, G. Primordial Nucleosynthesis in the Precision Cosmology Era. *ARNPS* **2007**, *57*, 463–491.
25. Starobinskiĭ, A.A. Spectrum of relict gravitational radiation and the early state of the universe. *Soviet JET Physics Letters* **1979**, *30*, 682.
26. Guth, A.H. Inflationary universe: A possible solution to the horizon and flatness problems. *PRD* **1981**, *23*, 347–356.
27. Linde, A.D. A new inflationary universe scenario. *Physics Letters B* **1982**, *108*, 389–393.
28. Albrecht, A.; Steinhardt, P.J. Cosmology for GUT with Radiatively Induced Symmetry Breaking. *PRL* **1982**, *48*, 1220–1223.

29. Liddle, A.R. Observational tests of inflation. *arXiv:9910110* **1999**.
30. Smoot, G.F.; etal. Structure in the COBE Differential Microwave Radiometer First-Year Maps. *ApJL* **1992**, *396*, L1.
31. Spergel, D.N.; etal. First year WMAP observations: Determination of cosmological parameters. *ApJ. Suppl.* **2003**, *148*, 175–194.
32. Planck Collaboration. Planck 2018 results. VI. Cosmological parameters. *A& A* **2020**, *641*, A6.
33. Aiola, S.; etal. The Atacama Cosmology Telescope: DR4 maps and cosmological parameters. *JCAP* **2020**, *2020*, 047–047.
34. Dutcher, D.; etal. Measurements of the E-mode polarization and temperature-E-mode correlation of the CMB from SPT-3G 2018 data. *Phys. Rev. D* **2021**, *104*, 022003.
35. Efstathiou, G.; Sutherland, W.J.; Maddox, S.J. The cosmological constant and cold dark matter. *Nature* **1990**, *348*, 705–707.
36. Gaztanaga, E.; Baugh, C.M. Testing deprojection algorithms on mock angular catalogues: evidence for a break in the power spectrum. *MNRAS* **1998**, *294*, 229–244.
37. Gawiser, E.; Silk, J. Extracting Primordial Density Fluctuations. *Science* **1998**, *280*, 1405.
38. DES Collaboration. DES Year 3 results: Cosmological constraints from galaxy clustering and weak lensing. *PRD* **2022**, *105*, 023520.
39. Efstathiou, G.; Bond, J.R.; White, S.D.M. COBE background radiation anisotropies and large-scale structure in the universe. *MNRAS* **1992**, *258*, 1P–6P.
40. Fry, J.N.; Gaztanaga, E. Biasing and Hierarchical Statistics in Large-Scale Structure. *ApJ* **1993**, *413*, 447.
41. Gaztañaga, E.; Juszkiewicz, R. Gravity's Smoking Gun? *ApJl* **2001**, *558*, L1–L4.
42. Eisenstein, D.J.; Hu, W. Baryonic Features in the Matter Transfer Function. *ApJ* **1998**, *496*, 605–614.
43. Eisenstein, D.J.; etal. Detection of the Baryon Acoustic Peak in the Large-Scale Correlation Function of SDSS Luminous Red Galaxies. *ApJ* **2005**, *633*, 560–574.
44. Gaztañaga, E.; Cabré, A.; Hui, L. Clustering of luminous red galaxies - IV. Baryon acoustic peak in the line-of-sight direction and a direct measurement of H(z). *MNRAS* **2009**, *399*, 1663–1680.
45. Gaztañaga, E.; Miquel, R.; Sánchez, E. First Cosmological Constraints on Dark Energy from the Radial Baryon Acoustic Scale. *PRL* **2009**, *103*, 091302.
46. Davis, M.; Efstathiou, G.; Frenk, C.S.; White, S.D.M. The evolution of large-scale structure in a universe dominated by cold dark matter. *ApJ* **1985**, *292*, 371–394.
47. Zwicky, F. On the Masses of Nebulae and of Clusters of Nebulae. *ApJ* **1937**, *86*, 217.
48. Rubin, V.C.; Ford, W. Kent, J. Rotation of the Andromeda Nebula from a Spectroscopic Survey of Emission Regions. *ApJ* **1970**, *159*, 379.
49. Clowe, D.; Gonzalez, A.; Markevitch, M. Weak-Lensing Mass Reconstruction of the Interacting Cluster 1E 0657-558: Direct Evidence for the Existence of Dark Matter. *ApJ* **2004**, *604*, 596–603.
50. Feldman, H.; etal. An Estimate of Ω_m without Conventional Priors. *ApJL* **2003**, *596*, L131–L134.
51. Bertone, G.; Hooper, D.; Silk, J. Particle dark matter: evidence, candidates and constraints. *PhysRep* **2005**, *405*, 279–390.
52. Profumo, S.; Giani, L.; Piattella, O.F. An Introduction to Particle Dark Matter. *Universe* **2019**, *5*, 213.
53. Perlmutter, S.; etal. Measurements of Ω and Λ from 42 High-Redshift Supernovae. *ApJ* **1999**, *517*, 565–586.
54. Riess, A.G.; etal. Observational Evidence from Supernovae for an Accelerating Universe and a Cosmological Constant. *AJ* **1998**, *116*, 1009–1038.
55. Huterer, D.; Turner, M.S. Prospects for probing the dark energy via supernova distance measurements. *PRD* **1999**, *60*, 081301.
56. Einstein, A. Kosmologische Betrachtungen zur allgemeinen Relativitätstheorie. *S.K. Preußischen Akademie der W.* **1917**, pp. 142–152.
57. Weinberg, S. The cosmological constant problem. *Reviews of Modern Physics* **1989**, *61*, 1–23.
58. Carroll, S.M.; Press, W.H.; Turner, E.L. The cosmological constant. *ARAA* **1992**, *30*, 499–542.
59. Peebles, P.J.; Ratra, B. The cosmological constant and dark energy. *Reviews of Modern Physics* **2003**, *75*, 559–606.
60. Crittenden, R.G.; Turok, N. Looking for a Cosmological Constant with the Rees-Sciama Effect. *PRL* **1996**, *76*, 575–578.
61. Gaztañaga, E.; Manera, M.; Multamäki, T. New light on dark cosmos. *MNRAS* **2006**, *365*, 171–177.
62. Ellis, G.F.R.; Rothman, T. Lost horizons. *American Journal of Physics* **1993**, *61*, 883–893.
63. Zel'Dovich, Y.B. Gravitational instability: an approximate theory for large density perturbations. *AAP* **1970**, *500*, 13–18.
64. Harrison, E.R. Fluctuations at the Threshold of Classical Cosmology. *PRD* **1970**, *1*, 2726–2730.
65. Peebles, P.J.E.; Yu, J.T. Primeval Adiabatic Perturbation in an Expanding Universe. *ApJ* **1970**, *162*, 815.
66. Bernardeau, F.; Colombi, S.; Gaztañaga, E.; Scoccimarro, R. Large-scale structure of the Universe and cosmological perturbation theory. *PhysRep* **2002**, *367*, 1–248.
67. Bera, P.; Jones, D.I.; Andersson, N. Does elasticity stabilize a magnetic neutron star? *MNRAS* **2020**, *499*, 2636–2647.
68. Carretero, J.; Castander, F.J.; Gaztañaga, E.; Crocce, M.; Fosalba, P. An algorithm to build mock galaxy catalogues using MICE simulations. *MNRAS* **2015**, *447*, 646–670.
69. Carr, B.; Kühnel, F. Primordial Black Holes as Dark Matter: Recent Developments. *ARNPS* **2020**, *70*, 355–394.
70. Hinshaw, G.; etal. Two-Point Correlations in the COBE DMR Four-Year Anisotropy Maps. *ApJL* **1996**, *464*, L25.
71. Gaztañaga, E.; etal. Two-point anisotropies in WMAP and the cosmic quadrupole. *MNRAS* **2003**, *346*, 47–57.
72. Efstathiou, G.; Ma, Y.Z.; Hanson, D. Large-angle correlations in the cosmic microwave background. *MNRAS* **2010**, *407*, 2530–2542.
73. Schwarz, D.J.; Copi, C.J.; Huterer, D.; Starkman, G.D. CMB anomalies after Planck. *CQGra* **2016**, *33*, 184001.
74. York, J.W. Role of Conformal Three-Geometry in the Dynamics of Gravitation. *PRL* **1972**, *28*, 1082–1085.
75. Gibbons, G.W.; Hawking, S.W. Cosmological event horizons, thermodynamics, and particle creation. *PRD* **1977**, *15*, 2738–2751.
76. Hawking, S.W.; Horowitz, G.T. The gravitational Hamiltonian, action, entropy and surface terms. *Class Quantum Gravity* **1996**, *13*, 1487–1498.

Preprints (www.preprints.org) | NOT PEER-REVIEWED | Posted: 31 January 2022 doi:10.20944/preprints202201.0459.v1

77. Mitra, A. Interpretational conflicts between the static and non-static forms of the de Sitter metric. *Nature Sci. Reports* **2012**, *2*, 923.
78. Easson, D.A.; Brandenberger, R.H. Universe generation from black hole interiors. *J. of High Energy Phy.* **2001**, *2001*, 024.
79. Daghigh, R.G.; Kapusta, J.I.; Hosotani, Y. False Vacuum Black Holes and Universes. *arXiv:gr-qc/0008006* **2000**.
80. Firouzjahi, H. Primordial Universe Inside the Black Hole and Inflation. *arXiv* **2016**, p. arXiv:1610.03767.
81. Oshita, N.; Yokoyama, J. Creation of an inflationary universe out of a black hole. *Physics Letters B* **2018**, *785*, 197–200.
82. Dymnikova, I. Universes Inside a Black Hole with the de Sitter Interior. *Universe* **2019**, *5*, 111.
83. Blau, S.K.; Guendelman, E.I.; Guth, A.H. Dynamics of false-vacuum bubbles. *PRD* **1987**, *35*, 1747–1766.
84. Frolov, V.P.; Markov, M.A.; Mukhanov, V.F. Through a black hole into a new universe? *Phys Let B* **1989**, *216*, 272–276.
85. Aguirre, A.; Johnson, M.C. Dynamics and instability of false vacuum bubbles. *PRD* **2005**, *72*, 103525.
86. Mazur, P.O.; Mottola, E. Surface tension and negative pressure interior of a non-singular 'black hole'. *CQGra* **2015**, *32*, 215024.
87. Garriga, J.; Vilenkin, A.; Zhang, J. Black holes and the multiverse. *JCAP* **2016**, *2016*, 064.
88. Kusenko, A.e. Exploring Primordial Black Holes from the Multiverse with Optical Telescopes. *PRL* **2020**, *125*, 181304.
89. Pathria, R.K. The Universe as a Black Hole. *Nature* **1972**, *240*, 298–299.
90. Good, I.J. Chinese universes. *Physics Today* **1972**, *25*, 15.
91. Popławski, N. Universe in a Black Hole in Einstein-Cartan Gravity. *ApJ* **2016**, *832*, 96.
92. Zhang, T.X. The Principles and Laws of Black Hole Universe. *Journal of Modern Physics* **2018**, *9*, 1838–1865.
93. Smolin, L. Quantization of unimodular gravity and the cosmological constant problems. *PRD* **2009**, *80*, 084003.
94. Knutsen, H. The idea of the universe as a black hole revisited. *Gravitation and Cosmology* **2009**, *15*, 273–277.
95. Stuckey, W.M. The observable universe inside a black hole. *American Journal of Physics* **1994**, *62*, 788–795.
96. Riess, A.G. The expansion of the Universe is faster than expected. *Nature Reviews Physics* **2019**, *2*, 10–12.
97. Di Valentino, E.; etal. In the realm of the Hubble tension-a review of solutions. *CQGra* **2021**, *38*, 153001.
98. Castelvecchi, D. How fast is the Universe expanding? Cosmologists just got more confused. *Nature* **2019**, *571*, 458–459.
99. Smolin, L. Did the Universe evolve? *CQGra* **1992**, *9*, 173–191.
100. Penrose, R. Gravitational Collapse and Space-Time Singularities. *Phys. Rev. Lett.* **1965**, *14*, 57–59.
101. Dadhich, N. Singularity: Raychaudhuri equation once again. *Pramana* **2007**, *69*, 23.
102. Ellis, G. Opposing the multiverse. *Astronomy and Geophysics* **2008**, *49*, 2.33–2.35.
103. Padmanabhan, T. *Gravitation, Cambridge Univ. Press*; 2010.
104. Israel, W. Singular hypersurfaces and thin shells in general relativity. *Nuovo Cimento B Serie* **1967**, *48*, 463–463.
105. Barrabès, C.; Israel, W. Thin shells in general relativity and cosmology: The lightlike limit. *PRD* **1991**, *43*, 1129–1142.
106. Hilbert, D. Die Grundlage der Physick. *Konigl. Gesell. d. Wiss. Göttingen, Math-Phys K* **1915**, *3*, 395–407.
107. Landau, L.D.; Lifshitz, E.M. *The classical theory of fields*; 1971.
108. Carroll, S.M. *Spacetime and geometry. Addison-Wesley,*; 2004.
109. Kerr, R.P. Gravitational Field of a Spinning Mass as an Example of Algebraically Special Metrics. *PRL* **1963**, *11*, 237–238.

Appendix A Exact solution in General Relativity

The flat FLRW metric in comoving coordinates $\xi^\alpha = (\tau, \chi, \theta, \delta)$, corresponds to an homogeneous and isotropic space:

$$ds^2 = f_{\alpha\beta} d\xi^\alpha d\xi^\beta = -d\tau^2 + a(\tau)^2 \left[d\chi^2 + \chi^2 d\Omega \right] \tag{A10}$$

where we have introduced the solid angle: $d\Omega^2 = d\theta^2 + \sin\theta^2 d\delta^2$. The scale factor, $a(\tau)$, describes the expansion/contraction as a function of comoving or cosmic time τ (proper time for a comoving observer). For a perfect fluid Eq.A33 with density ρ and pressure p, the solution to Einstein's field equations Eq.A32 is well known [103]:

$$H^2 \equiv \left(\frac{\dot{a}}{a}\right)^2 = \frac{8\pi G}{3}\rho = H_0^2 \left[\Omega_m a^{-3} + \Omega_R a^{-4} + \Omega_\Lambda \right] \tag{A11}$$

$$\rho_\Lambda \equiv \rho_{\rm vac} + \frac{\Lambda}{8\pi G} \quad ; \quad \rho_c \equiv \frac{3H^2}{8\pi G} \quad ; \quad \Omega_X \equiv \frac{\rho_X}{\rho_c(a=1)} \tag{A12}$$

where Ω_m (or ρ_m) represent the matter density today ($a = 1$), Ω_R is the radiation, $\rho_{\rm vac}$ represents vacuum energy: $\rho_{\rm vac} = -p_{\rm vac} = V(\varphi)$ and $\rho_\Lambda = -p_\Lambda$ is the effective cosmological constant density. Note that Λ (the raw value) is always constant, but ρ_Λ (effective value) can change if ρ_{vac} changes. Given $\rho(\tau)$ and $p(\tau)$ we can use the above equations to find $a(\tau)$.

Consider next the most general form of a metric with spherical symmetry in physical or Schwarzschild (SW) coordinates (t, r, θ, φ) [1,103]:

$$ds^2 = g_{\mu\nu} dx^\mu dx^\nu = -(1+2\Psi)dt^2 + \frac{dr^2}{1+2\Phi} + r^2 d\Omega^2 \tag{A13}$$

Preprints (www.preprints.org) | NOT PEER-REVIEWED | Posted: 31 January 2022 doi:10.20944/preprints202201.0459.v1

where $\Phi = \Phi(t,r)$ and $\Psi = \Phi(t,r)$ are the generic gravitational potentials. The Weyl potential Φ_W is the geometric mean of the two:

$$(1+2\Phi_W)^2 = (1+2\Phi)(1+2\Psi) \tag{A14}$$

Ψ describes propagation of non-relativist particles and Φ_W the propagation of light. The solution to Einstein's field equations Eq.A32 for empty space ($\rho = p = \rho_\Lambda = 0$) results in the Schwarzschild (SW) metric:

$$2\Phi = 2\Psi = -2GM/r \equiv -r_S/r \tag{A15}$$

which describes a singular BH of mass M at $r = 0$. The solution for $\rho = p = M = 0$, but $\rho_\Lambda \neq 0$ results in deSitter (dS) metric:

$$2\Phi = 2\Psi = -r^2/r_\Lambda^2 \equiv -r^2 H_\Lambda^2 = -r^2 8\pi G\rho_\Lambda/3 \tag{A16}$$

We also consider a generalization of dS metric, which we call dS extension (dSE), which is just a recast of the general case:

$$2\Phi(t,r) \equiv -r^2 H^2(t,r) \equiv -r^2/r_H^2. \tag{A17}$$

and arbitrary Ψ.

Appendix A.1 Dual frame: FLRW in the physical frame

Consider a change of variables from $x^\mu = [t,r]$ to comoving coordinates $\xi^\nu = [\tau,\chi]$, where $r = a(\tau)\chi$ and angular variables (θ,δ) remain the same. The metric $g_{\mu\nu}$ in Eq.A13 transforms to $f_{\alpha\beta} = \Lambda^\mu_\alpha \Lambda^\nu_\beta g_{\mu\nu}$, with $\Lambda^\mu_\nu \equiv \frac{\partial x^\mu}{\partial \xi^\nu}$. If we use:

$$\Lambda = \begin{pmatrix} \partial_\tau t & \partial_\chi t \\ \partial_\tau r & \partial_\chi r \end{pmatrix} = \begin{pmatrix} (1+2\Phi_W)^{-1} & arH(1+2\Phi_W)^{-1} \\ rH & a \end{pmatrix} \tag{A18}$$

with $2\Phi = -r^2H^2$ and arbitrary $a(\tau)$ and Ψ, we find:

$$f_{\alpha\beta} = \Lambda^T \begin{pmatrix} -(1+2\Psi) & 0 \\ 0 & (1+2\Phi)^{-1} \end{pmatrix} \Lambda = \begin{pmatrix} -1 & 0 \\ 0 & a^2 \end{pmatrix} \tag{A19}$$

In other words, these two metrics are the same:

$$-(1+2\Psi)dt^2 + \frac{dr^2}{1-r^2H^2} = -d\tau^2 + a^2 d\chi^2 \tag{A20}$$

dSE metric in Eq.A17 with $2\Phi = -r^2H^2$ corresponds to the FLRW metric with $H(t,r) = H(\tau)$: this is a hypersphere of radius r_H that tends to r_Λ (see Fig.A6). This frame duality can be understood as a Lorentz contraction $\gamma = 1/\sqrt{1-u^2}$ where the velocity $u = \dot{r}$ is given by the expansion law: $\dot{r} = Hr$. An observer in the SW frame, not moving with the fluid, sees the moving fluid element $ad\chi$ contracted by the Lorentz factor γ: $ad\chi \Rightarrow \gamma dr$.

Appendix A.2 The BHU solution

We next look for solutions where we have matter $\rho_m = \rho_m(t,r)$ and radiation $\rho_R = \rho_R(t,r)$ inside some radius R and empty space outside:

$$\rho(t,r) \quad = \quad \begin{cases} 0 & \text{for } r > R \\ \rho_m + \rho_R & \text{for } r < R \end{cases}. \tag{A21}$$

When $R > r_S$ we call this a FLRW cloud and when $R < r_S$ this is a BH Universe. For $r > R$, we have the SW metric. For the interior we use the dSE notation in EqA17: $2\Phi(t,r) \equiv -r^2H^2(t,r) \equiv -r^2/r_H^2$, so that:

$$2\Phi(t,r) = \begin{cases} -r_S/r & \text{for } r > R \\ -r^2H^2 & \text{for } r < R \end{cases} \tag{A22}$$

At the junction $r = R$, we reproduce Eq.8. For $r < R$ we can change variables as in Eq.A18-A20. In the comoving frame of Eq.A20, from every point inside de BHU, comoving observers will have the illusion of an homogeneous and isotropic space-time around them,

Preprints (www.preprints.org) | NOT PEER-REVIEWED | Posted: 31 January 2022 doi:10.20944/preprints202201.0459.v1

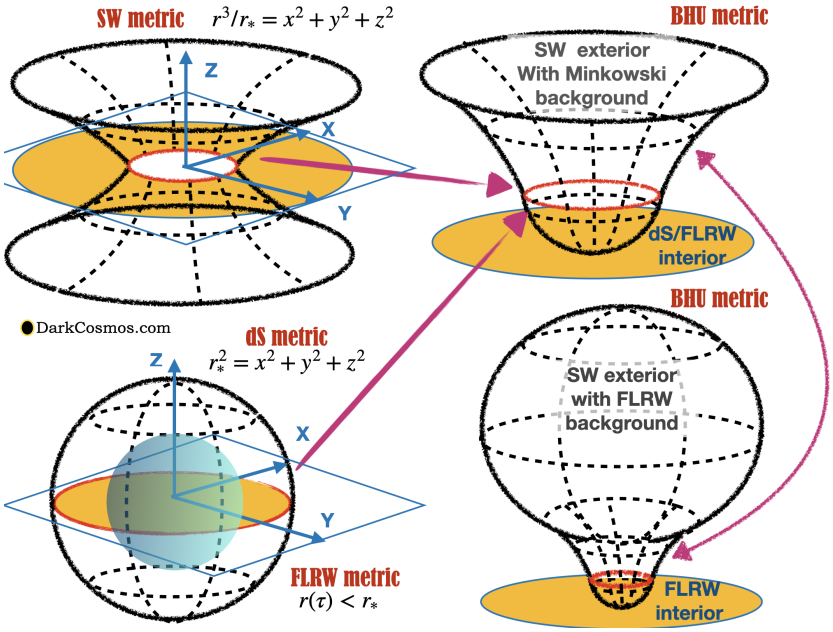

Figure A6. Representation of $ds^2 = (1+2\Phi)^{-1}dr^2 + r^2 d\theta^2$ in polar coordinates embedded in 3D flat space. Yellow region shows the 2D projection coverage in the true (x, y) plane. From bottom left clockwise we show: deSitter (dS, $2\Phi = -r^2/r_*^2$), FLRW ($r = r(\tau) < r_*$, blue sphere inside dS) and Schwarzschild (SW, $2\Phi = -r_*/r$). In the top right we show a BHU with dS (or FLRW) interior and SW exterior joint at the Event Horizon $r_* = 2GM = 1/H_\Lambda$ (red circles). More generally, the BHU solution has two nested FLRW metrics join by SW metric (bottom right).

with a fixed Hubble-Lemaitre expansion $H(\tau)$. This converts dSE metric into FLRW metric. So the solution is $H(t, r) = H(\tau)$ and $R(\tau) = [r_S/H^2(\tau)]^{1/3}$. Given $\rho(\tau)$ and $p(\tau)$ in the interior we can use Eq.A11 to find $H(\tau)$ and $R(\tau)$:

$$H^2(\tau) = \frac{8\pi G}{3}\rho(\tau) = \frac{r_S}{R^3(\tau)} \tag{A23}$$

This corresponds to a homogeneous FLRW cloud of fix mass $M = r_S/2G$ in Eq.2 and Eq.8. This solution exist for any content inside R [8]. Fig.A6 shows a spatial representation of the SW, dS, FLRW and BHU solutions.

Appendix A.3 Junction conditions

We can arrive at the same BHU solution using Israel's junction conditions ([104,105]). We can combine two solutions with different energy content, as in Eq.A21, to find a new solution. To do that we need to find an hypersurface junction Σ to match them well. In our case, this will be given by R. The junction conditions require that the metric and its derivative (the extrinsic curvature K) match at Σ. The join metric them provides a new solution to GR. In many cases, like in the Bubble Universes or gravastar [83–88], which match dS and SW metric, this does not work and the junction requires a surface term (the bubble) to glue both solutions together. For the BHU there are no surface terms[8] which shows that this is an exact solution. In the limit where the FLRW has constant H (i.e our future), the BHU solution corresponds to match between dS and SW metric. So a Bubble Universe without bubble.

To see this consider the case where Σ is given by R in the freefall collapse of a FLRW cloud of fixed mass M. For matter domination this corresponds to $R = a(\tau)\chi_*$ as in Eq.8, where $\chi_* = r_S/a_{BH}$ is fixed. The induced 3D metric on Σ is $h^-_{\alpha\beta}$ with coordinates $dy^\alpha = (d\tau, d\delta, d\theta)$:

$$ds^2_{\Sigma^-} = h^-_{\alpha\beta}dy^\alpha dy^\beta = -d\tau^2 + a^2(\tau)\chi_*^2 d\Omega^2 \tag{A24}$$

For the outside SW frame, the junction Σ^+ is described by $r = R(\tau)$ and $t = T(\tau)$, where τ is the FLRW comoving time and t the time in the physical frame. We then have:

$$dr = \dot{R}d\tau \;\; ; \;\; dt = \dot{T}d\tau, \tag{A25}$$

where the dot refers to derivatives with respect to τ. The metric h^+ induced in the outside SW metric is:

$$\begin{aligned} ds^2_{\Sigma^+} &= h^+_{\alpha\beta}dy^\alpha dy^\beta = -F dt^2 + \frac{dr^2}{F} + r^2 d\Omega^2 \\ &= -(F\dot{T}^2 - \dot{R}^2/F)d\tau^2 + R^2 d\Omega^2 \end{aligned} \tag{A26}$$

Preprints (www.preprints.org) | NOT PEER-REVIEWED | Posted: 31 January 2022 doi:10.20944/preprints202201.0459.v1

where $F \equiv 1 - r_S/R$. Comparing Eq.A24 with Eq.A26, the first matching conditions $h^- = h^+$ are then:

$$R(\tau) = a(\tau)\chi_* \;\; ; \;\; F\dot{T} = \sqrt{\dot{R}^2 + F} \equiv \beta(R, \dot{R}) \tag{A27}$$

For any given $a(\tau)$ and χ_* we can find both $R(\tau)$ and $\beta(\tau)$. We also want the derivative of the metric to be continuous at Σ. For this, we estimate the extrinsic curvature $K^\pm$ normal to $\Sigma^\pm$ from each side of the hypersurface:

$$K_{\alpha\beta} = -\left[\partial_a n_b - n_c \Gamma^c_{ab}\right] e^a_\alpha e^b_\beta \tag{A28}$$

where $e^a_\alpha = \partial x^a / \partial y^\alpha$ and n_a is the 4D vector normal to Σ. The outward 4D velocity is $u^a = e^a_\tau = (1, 0, 0, 0)$ and the normal to Σ^- on the inside is then $n^- = (0, a, 0, 0)$. On the outside $u^a = (\dot{T}, \dot{R}, 0, 0)$ and $n^+ = (-\dot{R}, \dot{T}, 0, 0)$. It is straightforward to verify that: $n_a u^a = 0$ and $n_a n^a = +1$ (for a timelike surface) for both n^- and n^+. We then find that the extrinsic curvature in Eq.A28 to the Σ junction, estimated with the inside FLRW metric, i.e. K^- is:

$$\begin{aligned} K^-_{\tau\tau} &= -(\partial_\tau n^-_\tau - a\Gamma^\chi_{\tau\tau}) e^\tau_\tau e^\tau_\tau = 0 \\ K^-_{\theta\theta} &= a\Gamma^\chi_{\theta\theta} e^\theta_\theta e^\theta_\theta = -a\chi_* = -R \end{aligned} \tag{A29}$$

For the SW metric:

$$\begin{aligned} K^+_{\tau\tau} &= \ddot{R}\dot{T} - \dot{R}\ddot{T} + \frac{\dot{T} r_S}{2R^2 F}(\dot{T}^2 F^2 - 3\dot{R}^2) = \frac{\dot{\beta}}{\dot{R}} \\ K^+_{\theta\theta} &= \dot{T}\Gamma^r_{\theta\theta} = -\dot{T} F R = -\beta R \end{aligned} \tag{A30}$$

where we have used the definition of β in Eq.A27. In both cases $K_{\delta\delta} = \sin^2\theta K_{\theta\theta}$, so that when $K^-_{\theta\theta} = K^+_{\theta\theta}$ it follows that $K^-_{\delta\delta} = K^+_{\delta\delta}$. Comparing Eq.A29 with Eq.A30, the matching conditions $K^-_{\alpha\beta} = K^+_{\alpha\beta}$ require $\beta = 1$, which using Eq.A27 gives:$R = \left[r_H^2 r_S\right]^{1/3}$. This reproduces the junction in Eq.8. So the two metrics and derivatives (the extrinsic curvature) are identical in the hypersurface defined by R. This completes the proof that the FLRW cloud is an exact solution of GR without surface terms. For more detailes see [8].

Appendix B The Action of GR and the Λ term

Consider the Einstein-Hilbert action ([103,106]):

$$S = \int_{V_4} dV_4 \left[\frac{R - 2\Lambda}{16\pi G} + \mathcal{L}\right], \tag{A31}$$

where $dV_4 = \sqrt{-g}d^4x$ is the invariant volume element, V_4 is the volume of the 4D spacetime manifold, $R = R^\mu_\mu = g^{\mu\nu}R_{\mu\nu}$ is the Ricci scalar curvature and $\mathcal{L}$ the Lagrangian of the energy-matter content. We can obtain Einstein's field equations (EFE) for the metric field $g_{\mu\nu}$ from this action by requiring S to be stationary $\delta S = 0$ under arbitrary variations of the metric $\delta g^{\mu\nu}$. The solution is ([18,103]):

$$G_{\mu\nu} + \Lambda g_{\mu\nu} = 8\pi G\, T_{\mu\nu} \equiv -\frac{16\pi G}{\sqrt{-g}} \frac{\delta(\sqrt{-g}\mathcal{L})}{\delta g^{\mu\nu}}, \tag{A32}$$

where $G_{\mu\nu} \equiv R_{\mu\nu} - \frac{1}{2} g_{\mu\nu} R$. For perfect fluid in spherical coordinates:

$$T_{\mu\nu} = (\rho + p) u_\mu u_\nu + p g_{\mu\nu} \tag{A33}$$

where ρ, and p are the energy-matter density and pressure. This fluid can be made of several components, each with a different equation of state $p = \omega\rho$.

Eq.A32 requires that boundary terms vanish (e.g. see [103,107,108]). If there are boundaries to the dynamic equations, we need to add a Gibbons-Hawking-York (GHY) boundary term [74–76] to the action in Eq.A31:

$$S_{GHY} = \frac{1}{8\pi G} \oint_{\partial V_4} d^3y \sqrt{-h}\, K \tag{A34}$$

Preprints (www.preprints.org) | NOT PEER-REVIEWED | Posted: 31 January 2022 doi:10.20944/preprints202201.0459.v1

so that the total actions is $S + S_{GHY}$ and K is the trace of the extrinsic curvature at the boundary ∂V_4 and h is the induced metric. The expansion that happens inside an isolated BH is bounded by its event horizon $r < r_S$ and we need to add the GHY boundary term S_{GHY}. The integral is over the induced metric at ∂V_4, which for a time-like junction $d\chi = 0$ corresponds to $R = r_S$:

$$ds^2_{\partial V_4} = h_{\alpha\beta} dy^\alpha dy^\beta = -d\tau^2 + r_S^2 d\Omega^2 \tag{A35}$$

So the only remaing degrees of freedom in the action are time τ and the angular coordinates. We can use this metric and the trace of the extrinsic curvature at $R = r_S$ to estimate $K = -2/r_S$ from Eq.A29. This result is also valid for a null geodesic [8]. We then have:

$$S_{GHY} = \frac{1}{8\pi G} \int d\tau \, 4\pi r_S^2 \, K = -\frac{r_S}{G}\tau \tag{A36}$$

The Λ contribution to the action in Eq.A31 is: $S_\Lambda = -\Lambda V_4/(8\pi G) = -r_S^3 \Lambda \tau / 3G$ where we have estimated the total 4D volume V_4 as that bounded by ∂V_4 inside $r < r_S$. i.e.: $V_4 = 2V_3\tau$, where the factor 2 accounts for the fact that $V_3 = 4\pi r_S^3/3$ is covered twice, first during collapse and again during expansion. Comparing the two terms we can see that we need $\Lambda = 3r_S^{-2}$ or equivalently $r_\Lambda = r_S$ to cancel the boundary term. In other words: evolution inside a BH event horizon induces a Λ term in the EFE even when there is no Λ term to start with. Such event horizon becomes a boundary for outgoing geodesics, i.e. expanding solutions. This provides a fundamental interpretation to the observed Λ as a causal boundary [5,6].

Appendix C Outside our BHU: a rotating cloud

If the FLRW cloud is not totally isolated it could have some rotation. This could be a way to infer if there is something outside our BHU. Any rotation, no matter how small, could prevent or interfere with the cloud collapse. Can we detect such rotation? A rotating BH is a bit more difficult to model because spherical symmetry is lost and the BH becomes oblate (i.e. the Kerr metric [109]):

$$x = \sqrt{r^2 + r_J^2} \sin\theta \cos\Phi \quad ; \quad y = \sqrt{r^2 + r_J^2} \sin\theta \cos\Phi \quad ; \quad z = r\cos\theta \tag{A37}$$

where $r_J = J/M$ is the ratio between the angular momentum J and the BH mass. A detailed analysis of this case is outside the scope of this review, but we will make some energetic considerations to understand the possible impact of such rotation on the Big Bounce. We assume that both mass M and angular momentum J are conserved, so r_J is constant. We also assume that $r_J \ll r_S$ so during the collapse we can neglect deviations from spherical symmetry. If we start from the FLRW cloud of size R and mass M with some small initial rotation, $\dot\theta$:

$$\frac{J}{M} = r_J = R^2\dot\theta = r_S^2 \dot\theta_{BH} \tag{A38}$$

As R gets smaller, $\dot\theta$ will become larger. The kinetic energy term in Eq.1 will have another contribution $2K = \dot R^2 + \dot\theta^2 R^2$, so that Eq.2 becomes:

$$r_H^{-2} \equiv H^2(\tau) = \frac{8\pi G}{3}\rho(\tau) - \frac{r_J^2}{R^4} = r_S^{-2}\left(\frac{a}{a_{BH}}\right)^{-3(1+\omega)} - \frac{r_J^2}{r_S^4}\left(\frac{a}{a_{BH}}\right)^{-4(1+\omega)} \tag{A39}$$

where in the last step we have used Eq.8 and Eq.3 for a collapsing FLRW cloud with equation of state ω. So rotation acts like a radiation term of negative energy density. Rotation is negligible, except when $a \Rightarrow 0$ when rotation tends to delay the collapse, as it reduces the expansion rate H. Unless angular momentum is lost some other way, the rotation component will dominate (stop the collapse) for:

$$r_J \simeq r_S \left(\frac{a}{a_{BH}}\right)^{(1+\omega)/2} \tag{A40}$$

Closed to the Big Bounce, when radiation dominates ($\omega = 1/3$) with neutron energy densities (GeV) we have $a \simeq 10^{-12} a_{BH}$. So the condition for the rotation not to interfere with the collapse is:

$$r_J \ll 10^{-8} r_S \tag{A41}$$

Equivalently, as $r_S \simeq H_0^{-1}$ (see Eq.7), $\dot\theta_{BH}$ in Eq.A38 has to be

$$\dot\theta_{BH} \ll 10^{-8} H_0 \tag{A42}$$

so less than 10^{-8} cycles per Hubble time. Such small contribution is undetectable in today's expansion law ($\Omega_J \simeq 10^{-16}$ in Eq.A39) or during recombination, but it could be bounded using Nucleosynthesis or affect the Big Bounce.